Zeeman splitting and spin dynamics tuning by exciton charging in two-dimensional systems

Leonardo K. Castelano,[*] Daniel Ferreira Cesar, Victor Lopez-Richard, and Gilmar E. Marques

Departamento de Física, Universidade Federal de São Carlos, 13565-905, São Carlos, São Paulo, Brazil

Odilon D. D. Couto Jr. and Fernando Iikawa

Instituto de Física "Gleb Wataghin", Universidade Estadual de Campinas, 13083-859, Campinas, São Paulo, Brazil

Rudolf Hey and Paulo V. Santos

Paul-Drude-Institut für Festkörperelektronik, Hausvogteiplatz 5-7, D-10117, Berlin, Germany

We report a study of magnetic responses of neutral and charged excitons in quantum wells, which are very sensitive to the strong spin hybridization of holes. This effect can be used to engineer the spin character of excitonic complexes in two-dimensional systems tuned by the magnetic field strength. Conditions for spin flip for each kind of excitonic complex is detailed and the nature of the effect discussed. Differences in the effective Zeeman splitting between neutral and charged excitons are theoretically predicted and unambiguously confirmed experimentally. Circularly polarized resolved photoluminescence has been used to study these effects under applied magnetic fields. The intertwining of spin dynamics of excitons and trions is discussed.

PACS number(s): 78.67.De, 85.75.−d, 71.35.Ji, 71.35.Pq

I. INTRODUCTION

The ability to perform spin operations is presently a driving force for different research endeavors. Within this scope, both neutral excitons (X^0)[1] and trions ($X^\pm$)[2–4] have been subjects of the experimental realization of fast spin control in two-dimensional (2D) systems. Thus, a clear understanding of the spin character of excitonic complexes under applied magnetic field becomes a relevant issue along with the need for an unambiguous identification of the complex nature. Recent observations of anomalous g-factor renormalization of trions[5,6] have highlighted several open issues and one of them is the elucidation of the nature of spin-dependent Coulomb interaction in 2D excitonic complexes. A systematic characterization of this effect was not previously available since the Zeeman splitting was considered unaffected in charged and neutral excitons. In this work, we investigate this mechanism in (110) semiconductor quantum wells (QWs) both theoretically and experimentally, and we identify conditions for effective tuning of the ground-state spin polarization of excitonic complexes by the magnetic field. We are able to report the photoluminescence (PL) confirmation of this effect enabling its generalization for 2D systems of different compositions. The nature of this behavior can be traced down to the strong valence band admixture in almost all semiconductors, as demonstrated in the forthcoming discussion.

For neutral excitons, the sub-band coupling and non-parabolicity of valence states become crucial factors determining the spin character of the quasiparticles under the presence of magnetic field. This statement is based on the fact that the total, as well as the z projection, of hole spins are no longer good quantum numbers for finite magnetic fields. The presence of extra charges within the trion configuration affects the spin hybridization and we conclude that these effects reveal detectable differences between neutral and charged excitons under magnetic fields. We confirm that both trion and exciton ground states may flip their spins at certain critical values of magnetic field strength and this effect

depends on the exciton charge as well. The mere presence of an extra electron in the negatively charged trion, X^-, may strongly affect the condition where such a spin flip may take place as shown theoretically and confirmed experimentally by magnetophotoluminescence (MPL). It has been reported that the spin polarization of trions in 2D systems can be tuned externally by the application of electromagnetic fields.[7] In this case, the effect of valence band spin hybridization has been discussed as a mere renormalization of the hole g factor.[8] We show in this work that the spin hybridization of the valence band may also lead to an asymmetry on the binding energy dependence on spin, an effect that has been neglected previously. An experimental characterization of the Landé factor tuning of excitons and trions in (001) GaAs QWs was performed in Ref. 5. These results also show the expected sign inversion of the Zeeman splitting by increasing magnetic field and the Coulomb renormalization of this effect, as simulated in our model. Analogous effects are expected in II-VI QWs, as already reported in Ref. 9.

The paper is organized as follows. In Sec. II, we introduce the theoretical model. Section III discusses the experimental results. Section IV presents the analysis of the spin dynamics of excitons and trions that enables the comprehension of the degree of circular polarization detected experimentally. Here, the contrasting behavior obtained experimentally for the spin dynamics of excitons and trions is explained. The concluding remarks are exposed in Sec. V.

II. THEORETICAL MODEL

Within the multiple carrier envelope function approximation, the Hamiltonian for the negative trion X^- in a field, $\mathbf{B} = (0,0,B)$, is given by[10]

$$
\begin{aligned}
H_{ij}^- = {} & H_{ij}^{\text{Lutt}}(\mathbf{k}_h) + E^{e1}(\mathbf{k}_{e1})\delta_{ij} \\
& + E^{e2}(\mathbf{k}_{e2})\delta_{ij} + [V_e(z_{e1}) + V_e(z_{e2}) + V_h(z_h)]\delta_{ij} \\
& + [V_C(\mathbf{r}_{e1} - \mathbf{r}_h) + V_C(\mathbf{r}_{e2} - \mathbf{r}_h) - V_C(\mathbf{r}_{e1} - \mathbf{r}_{e2})]\delta_{ij},
\end{aligned}
$$
(1)

TABLE I. Parameters used in the electronic structure calculations taken from Refs. 14–16.

GaAs parameters						
γ_1	γ_2	γ_3	κ	q	g_c	m_c
6.8	1.9	2.73	1.2	0.01	−0.45	0.067

where $H_{ij}^{\text{Lutt}}(\mathbf{k}_h)$ is the Luttinger Hamiltonian,[11] $E^e(\mathbf{k}_e)$ is the electron energy dispersion, V_e and V_h are square-well confinement potentials for electrons (e) and holes (h), respectively, and $V_C(\mathbf{r}) = -e^2/(\epsilon r)$ is the Coulomb interaction term. Also, we used the symmetric gauge $A = B/2(-y,x,0)$. When the dielectric properties of the well and barrier materials are similar, as we assume in this work, the effect of image charges can be neglected. For the neutral exciton X^0, the corresponding Hamiltonian is obtained by canceling one set of electron terms and for positive trions, X^+, an additional valence band Hamiltonian and all the corresponding extra-hole terms must be included in the X^0 Hamiltonian. In the finite magnetic field regime, when the Coulomb energy is smaller than the cyclotron energy of the free electron-hole pair, we are able to treat the Coulomb effect as a perturbation.

Here, the nonparabolicity of the energy bands is included in the binding energy calculation by using, as unperturbed states, the full Hamiltonian states without the Coulomb interaction. The Luttinger model used in these calculations corresponds mainly to the Hamiltonian for QWs grown along the [110] direction, which coincides with the growth direction of the sample used in the experiments. However, for sake of comparison, results corresponding to QWs grown along the direction [001] will also be presented. The electronic structure parameters used in the calculations are listed in Table I. The use of (110) QWs takes the advantage of the large spin lifetimes if compared with values for analogous systems grown along [001] direction.[12] For numerical diagonalization of the full Hamiltonian, we expand the envelope wave functions on a basis set composed by product of Landau-level functions of in-plane coordinates (r,θ) and QW functions along the z direction of the structure. For electrons, the single-particle basis can be written as

$$|l,n,m\rangle = F_l(z)\phi_{nm}(r)e^{i(n-m)\theta}. \tag{2}$$

Note that these electron quantum states are degenerate with respect to the azimuthal quantum number m. The basis for hole states can be obtained by simply switching the sign of θ coordinate. The radial wave function is given by

$$\phi_{nm}(r) = \frac{(-1)^{\min(n,m)}}{\sqrt{2\pi l_c^2}}\sqrt{\frac{\min(n,m)}{\max(n,m)}}\left(\frac{r}{\sqrt{2l_c^2}}\right)^{|n-m|}$$
$$\times e^{\frac{-r^2}{4l_c^2}}L_{\min(n,m)}^{|n-m|}\left(\frac{r^2}{2l_c^2}\right), \tag{3}$$

where L designates the generalized Laguerre polynomial functions and $l_c = \sqrt{\hbar c/eB}$ is the magnetic length. In the z-direction, we use the infinite QW barrier approximation that facilitates the analytical calculation of Coulomb matrix elements.[13] In this work, we consider only the Hartree term and disregard exchange effects.
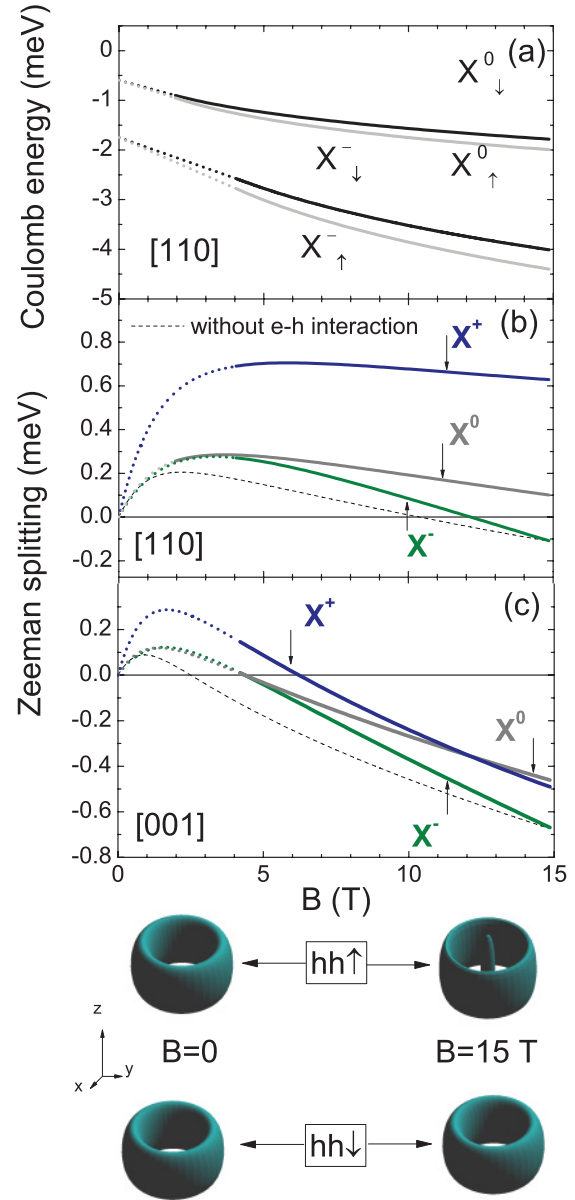
FIG. 1. (Color online) (a) Calculated Coulomb contribution to neutral exciton X^0 and trion X^- (ground state) binding energies vs magnetic field in a 23 nm (110) QW for two spin configurations indicated by vertical arrows. The dotted lines indicate the extrapolation of the Coulomb energy for zero magnetic field where the perturbation theory fails. (b) Calculated Zeeman splitting for optical recombination of X^0 and $X^\pm$ excitonic complexes in the (110) QW. The dotted lines correspond to the Zeeman splitting considering the extrapolated Coulomb energy. The dashed line curve shows the splitting for X^0 without Coulomb interaction. (c) Calculated Zeeman splitting for optical recombination of X^0 and $X^\pm$ excitonic complexes in a(001) QW. The lower panel shows the orbital shape for the $hh \uparrow hh \downarrow$ states with z component of the angular momentum $m = 2$ at magnetic fields $B = 0$ and $B = 15$ T.

Figure 1(a) shows the first-order perturbation energy correction due to Coulomb interaction for neutral and negatively charged excitons in the ground state considering different spin configurations. In the low magnetic field regime, where our perturbation expansion fails, we have extrapolated the values

from finite low fields toward the limit $B \rightarrow 0$ for illustrative reason (shown by dotted segments) and this procedure does not affect the main discussions. One can see that the Coulomb correction tuned by magnetic field strength depends on both the spin and the number of charges in the exciton complex. Neutral excitons and trions with spin-up configuration appear with higher energies than those with spin-down configurations. As expected, the absolute value for the Coulomb energy of negative trions (X^-) is larger than for neutral excitons (X^0). Such characteristics can be understood through the analysis of the unperturbed ground state wave functions, which can be written approximately as follows:

$$
\begin{aligned}
|\psi_e^{\uparrow,\downarrow}\rangle &\simeq |1,0,m_e\rangle |s\uparrow,\downarrow\rangle, \\
|\psi_h^{\downarrow}\rangle &\simeq |1,0,m_h\rangle |hh\downarrow\rangle, \\
|\psi_h^{\uparrow}\rangle &\simeq C_1|1,0,m_h\rangle |hh\uparrow\rangle + C_2|1,2,m_h\rangle |lh\downarrow\rangle \\
&\quad + C_3|2,1,m_h\rangle |lh\uparrow\rangle,
\end{aligned}
\tag{4}
$$

where $|\psi_e^{\uparrow,\downarrow}\rangle$ and $|\psi_h^{\uparrow,\downarrow}\rangle$ denote respectively the ground state wave function for electrons and holes with spin-up ($\uparrow$) and spin-down ($\downarrow$). The ground state wave functions are written as the product of envelope functions $|l,n,m\rangle$ and the usual Bloch functions $|s\downarrow\rangle,|s\uparrow\rangle,|hh\downarrow\rangle,|hh\uparrow\rangle,|lh\downarrow\rangle$, and $|lh\uparrow\rangle$. For electrons with spin-up and spin-down, the ground state wave functions only differ in the spin part of the Bloch function. The ground state wave function for spin-down holes remains almost pure as a function of the magnetic field and has the same envelope function as electrons. On the other hand, the ground state wave function for spin-up holes is composed of different Bloch functions, where the coefficients C_1, C_2, and C_3 are magnetic-field dependent. The hybridization tuning of the valence band ground state with magnetic field can be characterized spatially by the plots of the isoprobability surface displayed in the inset of Fig. 1 for the states with effective angular momentum $m = 2$ and $B = 0$ and 15 T. Note that a pure $m = 2$ orbital shows a ringlike structure at $B = 0$. This hybridization of different Bloch states is responsible for the difference between the Coulomb energy correction for complexes with different spins as a function of the magnetic field, because the matrix elements are obtained through the unperturbed wave functions. The Coulomb correction for electron-electron interaction and hole-hole interaction for spin-down holes gives practically the same result due to the similarity of the envelope functions. However, the electron-hole interaction contributes differently to X^- and X^0, twice for the former and once for the latter. Figure 1(b) shows the magnetic-field dependence of the Zeeman splitting for the X^-, X^+, and X^0 excitonic complexes. For comparison, the dashed curve in Fig. 1(b) shows the splitting for X^0 without considering the Coulomb interaction. The differences between calculated Coulomb corrections to the Zeeman splitting indicate the possibility of experimental identification of different types of exciton complexes: X^0, X^-, and X^+. For illustrative purpose, we show the analogous calculation for (001) QWs in Fig. 1(c). Although the main qualitative features are present in both Figs. 1(b) and 1(c), the effective mass anisotropy in the valence band and the Landau-level coupling dependence on direction lead to quantitative differences between both cases.

III. EXPERIMENTAL RESULTS

Our experimental study of these effects was carried out on a $GaAs/Al_{0.3}Ga_{0.7}As$ single QW, grown by molecular beam epitaxy on GaAs(110) substrate. The 18.2-nm thick QW was covered by 150-nm $Al_{0.3}Ga_{0.7}As$ and 10-nm GaAs. The MPL experiments were performed using an Ar-ion laser beam, line 514.5 nm, as the excitation source, which was focused on the sample using a $25\times$ objective lens placed inside a magnetocryostat. Same objective was used to collect the luminescence, which was analyzed in MPL experiments by a single monochromator coupled to a Si-CCD detector. The circular polarization of the luminescence was selected using a broadband 1/4 wave-plate retarder and a linear polarization analyzer. Figure 2 shows the MPL spectra vs excitation intensity. The increase of the excitation power leads to the appearance of the low-energy emission line ascribed to the trions X^-. The MPL spectrum can be well resolved for both circularly polarized emissions and the corresponding Zeeman splitting for both X^- and X^0 lines, as has been displayed in Fig. 3. The spectral analysis of these emissions allowed the characterization of the energy dispersion of the excitonic complexes with magnetic field as displayed in Figs. 4(a) and 4(b). At high magnetic fields a third emission line appears with polarization σ^+ attributed to an excited X_t^- triplet state.[9] Nevertheless, our discussion will focused on the X^0 and X^- ground states.

Figure 4(c) shows the Zeeman splitting taken from the σ^+ and σ^- emissions lines as a function of the magnetic field. We observe, as expected for QW, a nonlinear Zeeman splitting with magnetic field and the remarkable result is the quite different behavior of the energy splitting for two PL peaks assigned to X^0 and X^-. Both curves cross the magnetic-field axis for zero splitting in different points. This means that both excitons invert their ground states at different B. This inversion of spin
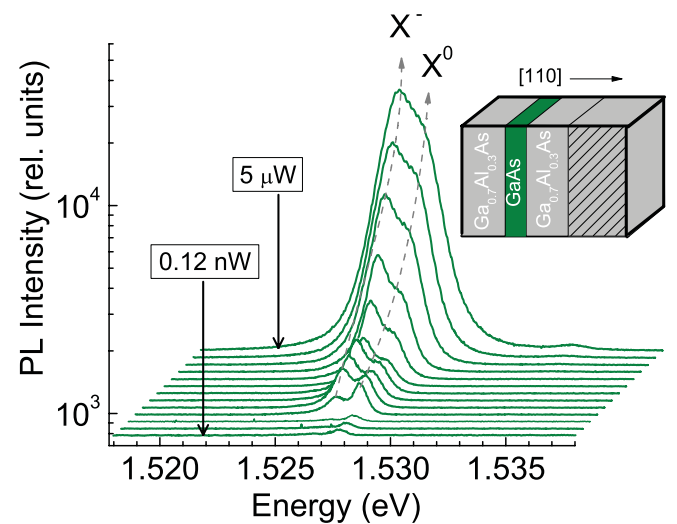
FIG. 2. (Color online) Magnetophotoluminescence taken at $T =$ 2 K for excitation power ranging from 0.12 nW to 5 μW. The enhancement of the lower-lying emission line with increasing power is ascribed to an increasing density of negatively charged trions (X^-) and, consequently, the decreasing numbers of neutral excitons (X^0). The inset illustrates the structure of the GaAs/AlGaAs (110) QWs.
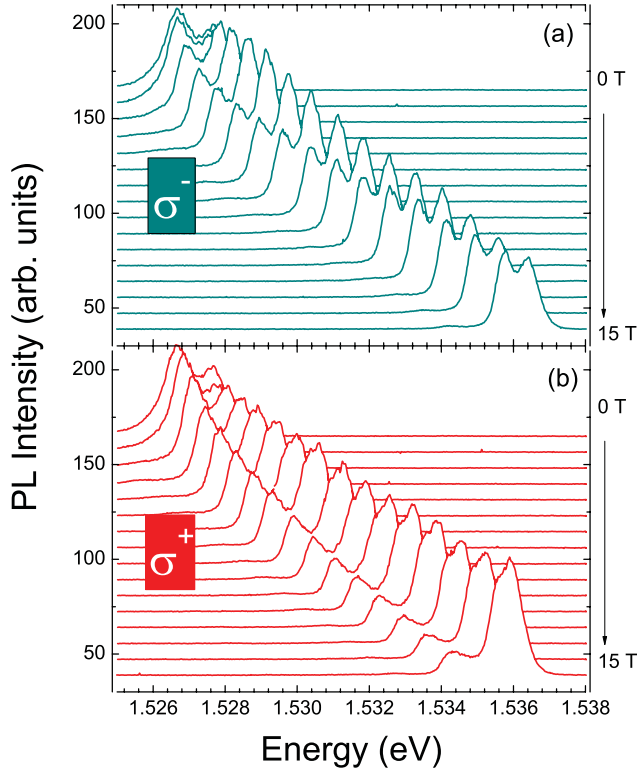
FIG. 3. (Color online) Magnetophotoluminescence spectra for different values of the magnetic field at $T = 2$ K and for excitation power of 5 nW: (a) for σ^- and (b) for σ^+ polarized emissions.

for each exciton may affect the population of the two spin states. In fact, the PL intensities of σ^+ and σ^-, shown in Fig. 3, oscillate with B. The discussion on this point will be shown in the next section. The distinct behavior of the Zeeman splitting shown in Fig. 4(c) between trion and neutral exciton is predicted in our model [Fig. 1(b)]. The signal inversion of the splitting energy for X^- occurs for lower B as compared to that for X^0, in agreement with the theoretical model. Quantitatively the order of the magnitude obtained by our calculations is also in reasonable agreement with the experimental data.

IV. CIRCULAR POLARIZATION

The tuning of the population imbalance of two spin states can be characterized by the degree of circular polarization (DCP). Given the integrated intensity of the spectral lines $I(\sigma^+)$ and $I(\sigma^-)$ of each complex, the DCP was obtained as

$$\text{DCP} = \frac{I(\sigma^+) - I(\sigma^-)}{I(\sigma^+) + I(\sigma^-)}. \tag{5}$$

The experimental values of the DCP obtained from the PL spectra for X^0 and X^- are plotted in the Fig. 4(d). The curves of two exciton complexes present opposite signals and both curves invert the polarity at different B, which corresponds to similar B where the Zeeman splitting data [Fig. 4(c)] crosses zero. To understand the behavior of the DCP vs magnetic field shown in Fig. 4(d), we calculate DCP based on the carrier dynamics of each exciton.
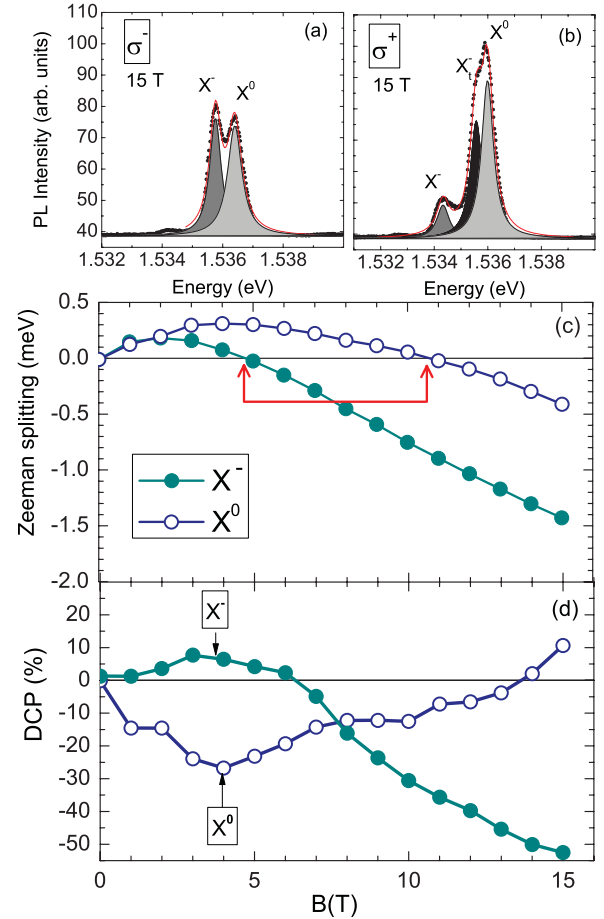
FIG. 4. (Color online) Spectral analysis of the magnetophotoluminescence spectra at $B = 15$ T for: (a) σ^- emissions and (b) σ^+ emissions. (c) Zeeman splitting of X^0 and X^- complexes as a function of the applied magnetic field extracted from the spectral analysis of the circularly polarized emissions. The critical magnetic field values where spin-inversion occurs are indicated. (d) Degree of circular polarization extracted from the PL spectra: open and filled circles correspond to the polarization of X^0 and X^- complexes, respectively.

To simulate the relative occupation of the spin-split states we have combined the electronic structure calculation described before with a dynamic model for the spin relaxation.[17,18] For X^0, the spin occupation, for spin generation rates, P_+ and P_-, at a temperature, T, follows the rate equations

$$P_+ = \frac{n_+}{\tau} + \frac{n_+}{\tau_s} - \frac{n_-}{\tau_s} \exp\left(-\frac{\Delta E}{k_B T}\right)$$
$$P_- = \frac{n_-}{\tau} - \frac{n_+}{\tau_s} + \frac{n_-}{\tau_s} \exp\left(-\frac{\Delta E}{k_B T}\right), \tag{6}$$

where n_+ and n_- denote the spin occupation of higher and lower energies, respectively (with $\Delta E = E_+ - E_- > 0$), τ is the optical recombination time, and τ_s the spin-relaxation time. In terms of the relative occupation of actual spin states, $n_\uparrow$ and $n_\downarrow$, the DCP can be calculated as DCP $= (\frac{n_\uparrow}{\tau} - \frac{n_\downarrow}{\tau})/(\frac{n_\uparrow}{\tau} + \frac{n_\downarrow}{\tau})$ and using Eq. (6), for equal spin generation rates $P_+ = P_-$

transforms to

$$\text{DCP} = \frac{\Delta E_{\uparrow\downarrow}}{|\Delta E_{\uparrow\downarrow}|} \frac{\exp\left(-\frac{|\Delta E_{\uparrow\downarrow}|}{k_B T}\right) - 1}{(1 + \tau_s/\tau) + \exp\left(-\frac{|\Delta E_{\uparrow\downarrow}|}{k_B T}\right)}, \quad (7)$$

with $\Delta E_{\uparrow\downarrow}$ the Zeeman splitting. This equation considers the possibility of the energy splitting sign inversion, confirmed both theoretically and experimentally. If the valence band hybridization tuning with magnetic field is considered, according to Eqs. (4), the term $n_\uparrow/\tau$ should be replaced by $|C_1(B)|^2 n_\uparrow/\tau$. This leads to a correction of the DCP as seen in Fig. 5 that demonstrates the relevance of this effect as the magnetic field increases. The result of introducing the calculated $C_1(B)$ and Zeeman splitting of the neutral exciton, X^0, into Eq. (7) is displayed in Fig. 5 where the parameters have been varied in order to assess their relative significance. Clearly, the oscillation of the DCP should be ascribed to the Zeeman splitting sign inversion. The ratio τ_s/τ influences the relative occupation of the spin-split states for a given temperature. In turn, the Coulomb interaction, responsible for the Zeeman splitting renormalization shifts the zero of the DCP to higher fields. For a given temperature, the nature of the predominant spin-relaxation process (and subsequently, the value of τ_s) depends on properties such as the effective carrier density and confinement size. Although no attempt for fitting the experimental results was performed, the parameter τ_s/τ in the simulation has been varied within a range that, for $\tau \sim 0.3$ ns,[19] corresponds to reported τ_s values under varying electron density conditions: $\tau_s \sim 0.3$ ns,[12,20] $\tau_s \sim 1.0$ ns[21] (according to the sample morphology and excitation conditions the optical recombination time can be increased to values $\tau \sim 1.0$ ns).[22] For a similar GaAs(110) QW sample to the one used in our experiments, with 20-nm thickness, grown under the same conditions in the same system, and measured at 20 K using magneto-Kerr rotation experiments (not shown), the values of $\tau_s = 2$ ns and $\tau = 2.3$ ns for neutral excitons were obtained. Since, the variation of both times between 2 to 20 K is expected to be negligible, this leads to a ratio $\tau_s/\tau \sim 1$. Thus, for this value, the population of neutral excitons follows the trends expected for spins that thermalize at $T = 2$ K that produce a DCP as obtained in Fig. 4(d).

In Fig. 4(d), the peculiar behavior of the trion X^- is also highlighted and, given the evolution of its Zeeman splitting with magnetic field [see Fig. 4(c)], the thermalizing dynamics that resulted in Eq. (7) cannot account for the trion DCP observed experimentally. In Ref. 9, a sign inversion of the trion DCP with respect to the neutral exciton was discussed in terms of a phenomenological model that considers an inversion of the relative positions of the Zeeman split states of both complexes. Although the sign of the $\Delta E_{\uparrow\downarrow}$ does not coincide, in the whole magnetic field range, for excitons and trions, this cannot be the cause of the DCP dependence on B obtained experimentally. The spin-relaxation dynamics, in the case of trions, appears linked to the simultaneous presence of excitons. Both complexes share the same source of carriers[23] thus their spin statistics should be intertwined. The statistics underneath the carriers dynamics and charge imbalance in the simultaneous occupation of exciton and trion states leads to the anomalous DCP of the trion X^-. At $B = 0$, one may assume the populations of electrons, n, holes, p, excitons, X^0, and
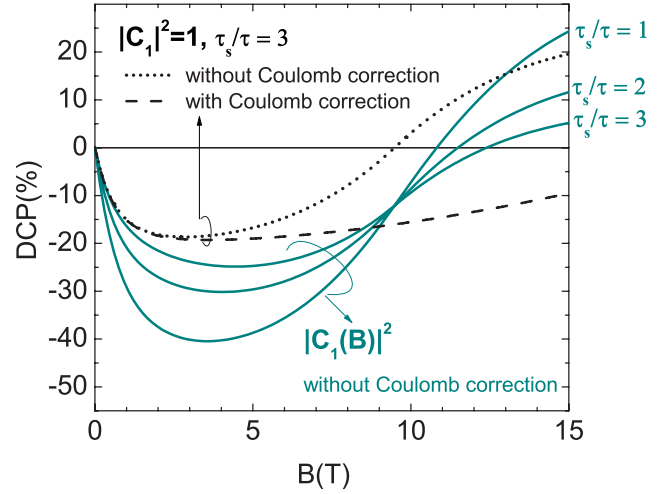
FIG. 5. (Color online) Theoretical calculations of the degree of circular polarization for the neutral exciton, X^0: dotted and dashed curves, without considering the valence band hybridization, and solid curves (considering the valence band hybridization tuning with magnetic field varying the parameter τ_s/τ within the range [1.0,3.0]).

trions, X^-, are governed by the equations[23]

$$\frac{dn}{dt} = P_e - P_0 n \cdot p - P_t n^2 p - P_i n \cdot X^0 + \frac{X^-}{\tau}, \quad (8)$$

$$\frac{dp}{dt} = P_h - P_0 n \cdot p - P_t n^2 p, \quad (9)$$

$$\frac{dX^0}{dt} = P_0 n \cdot p - \frac{X^0}{\tau} - P_i n \cdot X^0, \quad (10)$$

$$\frac{dX^-}{dt} = P_t n^2 \cdot p - \frac{X^-}{\tau} + P_i n \cdot X^0, \quad (11)$$

where $P_{e(h)}$ and $P_0 n \cdot p$ are the electron (hole) and exciton generation rates, while $P_t n^2 p$ and $P_i n \cdot X^0$ are the rates for the trion formation through the processes illustrated in the diagram displayed in Fig. 6. In the presence of a magnetic field, this dynamics can be complemented with the spin thermalization as introduced in Eq. (6) and the stationary equations for the spin-split states of each carrier become

$$P_e^+ = P_0 n_+ p_+ + P_t n_+^2 p_+ + P_i n_+ X_+^0 - \frac{X_+^-}{\tau}, \quad (12)$$

$$P_e^- = P_0 n_- p_- + P_t n_-^2 p_- + P_i n_- X_-^0 - \frac{X_-^-}{\tau}, \quad (13)$$

$$P_h^+ = P_0 n_+ p_+ + P_t n_+^2 p_+ + \frac{p_+}{\tau_s} - \frac{p_-}{\tau_s} e^{-\frac{\Delta E_h}{k_B T}}, \quad (14)$$

$$P_h^- = P_0 n_- p_- + P_t n_-^2 p_- - \frac{p_+}{\tau_s} + \frac{p_-}{\tau_s} e^{-\frac{\Delta E_h}{k_B T}}, \quad (15)$$

$$P_0 n_+ p_+ = \frac{X_+^0}{\tau} + P_i n_+ X_+^0 + \frac{X_+^0}{\tau_s} - \frac{X_-^0}{\tau_s} e^{-\frac{\Delta E_{X^0}}{k_B T}}, \quad (16)$$

$$P_0 n_- p_- = \frac{X_-^0}{\tau} + P_i n_- X_-^0 - \frac{X_+^0}{\tau_s} + \frac{X_-^0}{\tau_s} e^{-\frac{\Delta E_{X^0}}{k_B T}}, \quad (17)$$

$$P_t n_+^2 p_+ = \frac{X_+^-}{\tau} - P_i n_+ X_+^0 + \frac{X_+^-}{\tau_s} - \frac{X_-^-}{\tau_s} e^{-\frac{\Delta E_{X^-}}{k_B T}}, \quad (18)$$

$$P_t n_-^2 p_- = \frac{X_-^-}{\tau} - P_i n_- X_-^0 - \frac{X_+^-}{\tau_s} + \frac{X_-^-}{\tau_s} e^{-\frac{\Delta E_{X^-}}{k_B T}}. \quad (19)$$
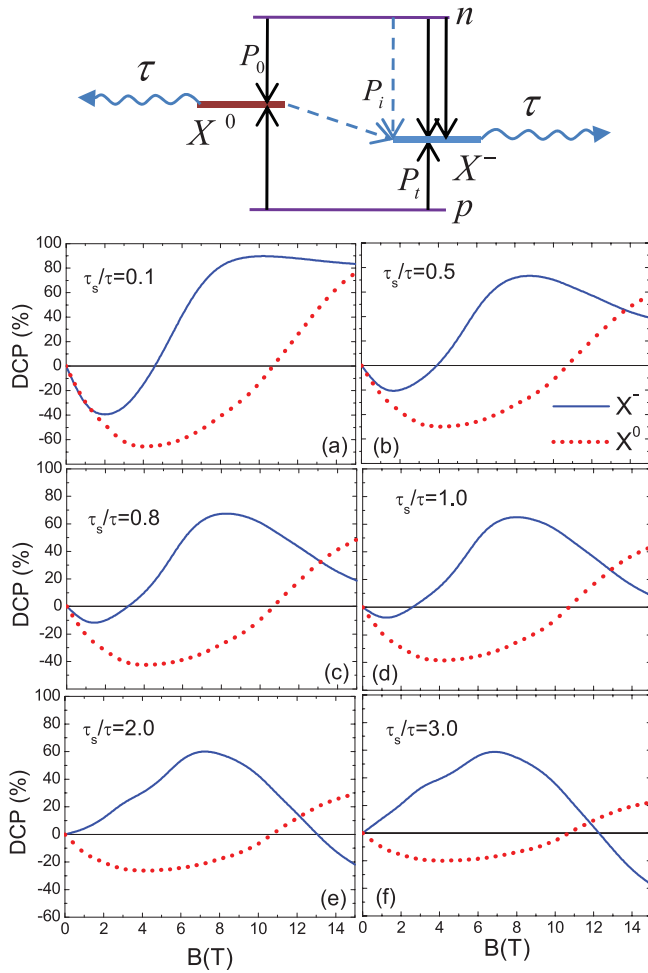
FIG. 6. (Color online) Upper panel: diagram representing the combined exciton and trion dynamics at $B = 0$ considered in the numerical simulations. (a)–(f) Theoretical calculations of the DCP for the neutral exciton, X^0 (dotted curves), and the trion, X^- (solid curves), as functions of the magnetic field by varying the parameter τ_s/τ within the range [0.1,3.0].

For simplicity, given the small value of the electron g factor, we have neglected the spin thermalization in the conduction band and the value of $g_c \mu_B B$. In the limit $P_e^+ = P_e^- \to P_h^+ = P_h^- = P$ these equations can be solved and the DCP for both trions and excitons obtained. We have considered a lower trion formation rate if compared to the exciton generation, $P_0/P_t = 100$, neglected the contribution of terms proportional to P_i, and varied the ratio τ_s/τ for assessing the DCP behavior of both excitons and trions between the limits of fast and slow spin relaxation. The Zeeman splittings of excitons and trions have been taken from the experimental values and the splitting of the holes calculated as $\Delta E_h \simeq \Delta E_{X^0}$ (since the electron Zeeman splitting was previously neglected).

The resulting pictures are displayed in Figs. 6(a)–6(f). Note, that for fast spin-relaxation times, $\tau_s/\tau = 0.1$, the DCP of both the excitons and trions responds as a thermalization given the different Zeeman splitting shown in Fig. 4(c). Yet, as τ_s/τ grows, the trion population tends to be governed by the spin density of the remaining carriers after the polarized excitons are formed and relaxed. In the limit of high τ_s/τ, a simplified reasoning can be set. From Eqs. (18) and (19), $\frac{X_{+(-)}^-}{\tau} \simeq P_t n_{+(-)}^2 p_{+(-)}$, and according to Eqs. (12) and (13), $P_t n_{+(-)}^2 p_{+(-)} \simeq P - P_0 n_{+(-)} p_{+(-)}$ yielding

$$\frac{X_{+(-)}^-}{\tau} \simeq P - P_0 n_{+(-)} p_{+(-)}. \tag{20}$$

In turn, from Eqs. (16) and (17), $P_0 n_{+(-)} p_{+(-)} \simeq \frac{X_{+(-)}^0}{\tau}$, thus the DCP of trions, $DCP_{X^-} \equiv (X_+^- - X_-^-)/(X_+^- + X_-^-)$, according to Eq. (20), becomes

$$DCP_{X^-} \simeq -(X_+^0 - X_-^0)/(X_+^- + X_-^-). \tag{21}$$

This leads to the sign inversion of the DCP of the trions if compared to the value obtained for excitons given by $DCP_{X^0} \equiv (X_+^0 - X_-^0)/(X_+^0 + X_-^0)$, as observed in the experimental results shown in Fig. 4(d).

V. CONCLUSION

In summary, under adequate structural parameters of 2D systems, the spin polarization of excitonic complexes can be effectively tuned by external magnetic field strength. The renormalization of the effective Zeeman splitting by charging the exciton is expected and confirmed. According to the field strength, the ground state spin polarization can be flipped and this condition differs for each kind of excitonic complex. This effect has been understood and traced down to the spin character of holes and the intersub-band coupling observed in the valence band of all semiconductors. The DCP of both excitons and trions has revealed the peculiar spin dynamics taking place in this kind of system. The neutral excitons are subjected to a spin thermalization, affected by the Zeeman splitting tuning with magnetic field, while the behavior of the trions, X^-, is affected by the spin population of the remaining carriers in the limit of slow spin-relaxation times. Given the dependence of the valence band spin hybridization on external bias and strain, as reported in Refs. 24 and 25, we are predicting that this effect can be easily tuned by an applied voltage and stress as well.

*lkcastelano@ufscar.br

[1] J. A. Gupta, R. Knobel, N. Samarth, and D. D. Awschalom, Science **292**, 2458 (2001).

[2] M. J. A. Schuetz, M. G. Moore, and C. Piermarocchi, Nat. Phys. **6**, 919 (2010).

[3] I. A. Yugova, A. A. Sokolova, D. R. Yakovlev, A. Greilich, D. Reuter, A. D. Wieck, and M. Bayer, Phys. Rev. Lett. **102**, 167402 (2009).

[4] C. Phelps, T. Sweeney, R. T. Cox, and H. Wang, Phys. Rev. Lett. **102**, 237402 (2009).

[5]S. Glasberg, G. Finkelstein, H. Shtrikman, and I. Bar-Joseph, Phys. Rev B **59**, R10425 (1999).

[6]V. Kochereshko, L. Besombes, H. Mariette, T. Wojtowicz, G. Karczewski, and J. Kossut, Phys. Status Solidi B **247**, 1531 (2010).

[7]R. I. Dzhioev, V. L. Korenev, M. V. Lazarev, V. F. Sapega, D. Gammon, and A. S. Bracker, Phys. Rev. B **75**, 033317 (2007).

[8]D. Andronikov, V. Kochereshko, A. Platonov, T. Barrick, S. A. Crooker, and G. Karczewski, Phys. Rev. B **72**, 165339 (2005).

[9]G. Bartsch, M. Gerbracht, D. R. Yakovlev, J. H. Blokland, P. C. M. Christianen, E. A. Zhukov, A. B. Dzyubenko, G. Karczewski, T. Wojtowicz, J. Kossut, J. C. Maan, and M. Bayer, Phys. Rev. B **83**, 235317 (2011).

[10]L. C. Andreani and A. Pasquarello, Phys. Rev. B **42**, 8928 (1990).

[11]G. Fishman, Phys. Rev. B **52**, 11132 (1995).

[12]Y. Ohno, R. Terauchi, T. Adachi, F. Matsukura, and H. Ohno, Phys. Rev. Lett. **83**, 4196 (1999).

[13]D. M. Whittaker and A. J. Shields, Phys. Rev. B **56**, 15185 (1997).

[14]K. Hess *et al.*, *Physics of Semiconductors: Proceedings of the 13th International Conference* (North-Holland, New York, 1976), p. 142.

[15]T. E. Ostromek, Phys. Rev. B **54**, 14467 (1996).

[16]Comprehensive Index, Landölt-Börnstein, New Series, edited by O. Madelung and W. Martienssen (Springer, Berlin, 1996).

[17]S. Mackowski, T. A. Nguyen, H. E. Jackson, L. M. Smith, J. Kossut, and G. Karczewski, Appl. Phys. Lett. **83**, 5524 (2003).

[18]E. Margapoti, L. Worschech, S. Mahapatra, K. Brunner, A. Forchel, Fabrizio M. Alves, V. Lopez-Richard, G. E. Marques, and C. Bougerol, Phys. Rev. B **77**, 073308 (2008).

[19]J. Martinez-Pastor, A. Vinattieri, L. Carraresi, M. Colocci, Ph. Roussignol, and G. Weimann, Phys. Rev. B **47**, 10456 (1993).

[20]S. Koh, K. Ikeda, and H. Kawaguchi, J. Appl. Phys. **110**, 043516 (2011).

[21]S. Döhrmann, D. Hägele, J. Rudolph, M. Bichler, D. Schuh, and M. Oestreich, Phys. Rev. Lett. **93**, 147405 (2004).

[22]N. Yokota, K. Ikeda, Y. Nishizaki, S. Koh, and H. Kawaguchi, IEEE Photonic. Tech. L. **22**, 1689 (2010).

[23]A. Vercik, Y. Galvão Gobato, I. Camps, G. E. Marques, M. J. S. P. Brasil, and S. S. Makler, Phys. Rev. B **71**, 075310 (2005).

[24]H. B. de Carvalho, M. J. S. P. Brasil, V. Lopez-Richard, Y. Galvao Gobato, G. E. Marques, I. Camps, L. C. O. Dacal, M. Henini, L. Eaves, and G. Hill, Phys. Rev. B **74**, 041305 (2006).

[25]D. F. Cesar, M. D. Teodoro, H. Tsuzuki, V. Lopez-Richard, G. E. Marques, J. P. Rino, S. A. Lourenço, E. Marega Jr., I. F. L. Dias, J. L. Duarte, P. P. González-Borrero, and G. J. Salamo, Phys. Rev. B **81**, 233301 (2010).